Self-assembled Framework Enhances Electronic Communication of Ultra-small Sized Nanoparticles for Exceptional Solar Hydrogen Evolution

Journal:	*Journal of the American Chemical Society*
Manuscript ID	ja-2016-12976b.R1
Manuscript Type:	Article
Date Submitted by the Author:	19-Feb-2017
Complete List of Authors:	Li, Xu-Bing; Technical Institute of Physics and Chemistry, Gao, Yu-Ji; Technical Institute of Physics and Chemistry, Wang, Yang; Technical Institute of Physics and Chemistry Zhan, Fei; Chinese Academy of Sciences, Chinese Academy of Sciences Zhang, Xiao-Yi; Argonne National Laboratory, X-ray Science Division Kong, Qingyu; Société civile Synchrotron SOLEIL, Zhao, Ning-Jiu; Renmin University of China, Department of Chemistry Guo, Qing; Technical Institute of Physics and Chemistry Wu, Hao-Lin; Technical Institute of Physics and Chemistry, CAS Li, Zhi-Jun; Technical Institute of Physics and Chemistry, Tao, Ye; Institute of High Energy Physics , Chinese Academy of Sciences Zhang, Jian-Ping; Renmin University of China, Department of Chemistry Chen, Bin; Chinese Academy of Sciences, Technical Institute of Physics and Chemistry Tung, Chen-Ho; Technical Institute of Physics and Chemistry, Chinese Academy of Sciences, Wu, Li-Zhu; Chinese Academy of Sciences, Technical Institute of Physics and Chemistry

Self-assembled Framework Enhances Electronic Communication of Ultra-small Sized Nanoparticles for Exceptional Solar Hydrogen Evolution

Xu-Bing Li,[†] Yu-Ji Gao,[†] Yang Wang,[†] Fei Zhan,[‡] Xiao-Yi Zhang, [§] Qing-Yu Kong,[ϟ] Ning-Jiu Zhao,[#] Qing Guo,[†] Hao-Lin Wu,[†] Zhi-Jun Li,[†] Ye Tao,[‡] Jian-Ping Zhang,[#] Bin Chen,[†] Chen-Ho Tung[†] & Li-Zhu Wu*[,†]

[†]Key Laboratory of Photochemical Conversion and Optoelectronic Materials, Technical Institute of Physics and Chemistry, Chinese Academy of Sciences, Beijing 100190, P. R. China
[‡]Beijing Synchrotron Radiation Facility, Institute of High Energy Physics, the Chinese Academy of Sciences Beijing 100049, P.R. China
[§]X-ray Sciences Division, Advanced Photon Source, Argonne National Laboratory, 9700 South Cass Avenue, Argonne, IL 60430, USA
[ϟ]Synchrotron Soleil, L'Orme des Merisiers St-Aubin, 91192 Gif-sur-Yvette Cedex, France
[#]Department of Chemistry, Renmin University of China, Beijing 100872, P.R. China

Supporting Information Placeholder

ABSTRACT: Colloidal quantum dots (QDs) have demonstrated great promise in artificial photosynthesis. However, the ultra-small size hinders its controllable and effective interaction with cocatalysts. To improve the poor interparticle electronic communication between free QD and cocatalyst, we design here a self-assembled architecture of nanoparticles, QDs and Pt-nanoparticles, simply jointed together by molecular polyacrylate to greatly enhance the rate and efficiency of interfacial electron transfer (ET). The enhanced interparticle electronic communication is confirmed by femtosecond transient absorption spectroscopy and X-ray transient absorption. Taking advantage of the enhanced interparticle ET with a time scale of ~65 ps, 5.0 mL assembled CdSe/CdS QDs/cocatalysts solution produces 94 ± 1.5 mL (4183 ± 67 μmol) molecular H_2 in 8 h, giving rise to an internal quantum yield of ~65% in the first 30 min and a total turnover number of >16,400,000 per Pt-nanoparticle. This study demonstrates that self-assembly is a promising way to improve the sluggish kinetics of interparticle ET process, which is the key step for advanced H_2 photosynthesis.

INTRODUCTION

Fascinated by the ability of natural photosynthesis to convert solar energy into chemical fuels, hydrogen (H_2) stored in a chemical form of reduced nicotinamide adenine dinucleotide phosphate (NADPH), the scientific community has been devoting considerable efforts to replicating the natural process.[1-14] Colloidal quantum dots (QDs) have recently appeared at the forefront and triggered a huge interest in the construction of artificial photocatalysts.[15-18] Taking advantages of the intrinsic characteristics in light response over a broad spectral range and the enhanced surface amplitude of photogenerated excitons, QDs have shown much higher activity for solar H_2 evolution than those of organic dyes, metal complexes, and bulk counterparts.[19-25] At the same time, the quantum confined QDs face the striking obstacle in the facile communication with cocatalysts because direct loading cocatalysts on QDs is limited by the extremely finite surface and surface elemental complexity, different types of crystallographic facets and high concentration of corner and edge sites, which most likely go against providing sufficient sites for binding cocatalysts. As a result, the interparticle electronic communication, *via* a diffusion-controlled electron transfer (ET) process[26,27] of an upper limit of ~10^{10} M^{-1} s^{-1}, between individually separated QD and cocatalyst becomes the bottleneck to take one step further toward advanced H_2 photosynthesis.

To overcome the sluggish electronic communication between individually separated QD and cocatalyst, electron mediator, such as methyl viologen (MV^{2+}),[28] TiO_2,[29] and graphene,[30] has been used as a shuttle for ET from QDs to cocatalysts. However, most of these systems exhibit moderate performance of solar H_2 evolution due to the low efficiency of subsequent electron transfer from the reduced mediator to cocatalyst. Alternatively, QDs have been directly incorporated with molecular cocatalysts (such as cobalt complex[31,32]

and [FeFe]-hydrogenase mimic[33]) or metal cocatalysts (such as Pt[34], Co[35] and Ni[36]) to achieve efficient photo-electron capture. However, this method suffers from charge recombination and formation of trap states on the surface of colloidal QDs, both of which provide extra pathways for exciton annihilation and heavily compromise the amelioration of solar H_2 evolution. Hence, the ability to assemble nanometer-sized QDs with cocatalysts in a controllable and friendly fashion would provide an effective way to break the diffusion-controlled charge transfer process for further improvement of solar H_2 evolution.

Toward this goal, we initiated a self-assembling way to fabricate assembled frameworks of QDs and Pt-nanoparticles for facile and ultra-fast interparticle electron transfer. In this contribution, the surface ligands, polyacrylate anions, are used to strongly bind light absorbers (QDs) and cocatalysts (Pt-nanoparticles) together to form the advanced architecture, which duplicates the structure and function of natural photosynthetic systems. In natural photosynthetic systems, light-absorbing chlorophylls are well organized to form light harvesting assemblies, and the primary light absorption and subsequent transfer of electronic excitation energy and electrons within the assemblies toward the reaction center are extremely important for the conversion of sunlight into chemical energy.[37,38] In the current study, the interparticle electronic communication between ultra-small particles of QDs and Pt is greatly enhanced. Femtosecond transient absorption (TA) spectroscopy and X-ray transient absorption (XTA) indicate that the interparticle electron transfer from QDs, for example CdSe/CdS QDs, to Pt-nanoparticle occurs in a time scale of ~65 ps, which overcomes the sluggish ET kinetics from surrounded QDs to subsequent catalytic reaction centers, just as nature does. For practically viable artificial photosynthetic systems, the assembled system, taking CdSe/CdS QDs as an example, can produce 94 ± 1.5 mL (4183 ± 67 μmol) H_2 gas in 8 h from 5.0 mL solution, giving an initial internal quantum yield of ~65% and a total turnover number (TON) of >16,400,000 per Pt-nanoparticle.

RESULTS AND DISCUSSION

Fabrication of the self-assembled architecture. To establish this proof-of-concept model of assembled frameworks for enhanced interparticle communication, colloidal CdSe/CdS QDs are selected for its advantages in visible-light response and charge separation, and typical Pt-nanoparticles are employed as proton reduction cocatalyst. First, sulfide stabilized CdSe/CdS QDs are obtained *via* a seeded-growth method of growing CdS shell on the surface of mercaptopropionic acid (MPA) stabilized CdSe QDs,[39,40] see details in Supporting Information. As presented in Figure 1a and Figure S1a, CdSe QDs are nearly spherical nanoparticles with a diameter of ~2.0 nm, while the obtained CdSe/CdS QDs give an ellipsoidal shape with a width of 2.5 ± 0.5 nm and a length of 4.5 ± 1.0 nm (Figure 1b and Figure S1b). Because of the small lattice mismatch (~4.0%),[41] it is hard to distinguish CdSe and CdS in the heterogeneous structure in transmission electron microscope (TEM). X-ray diffraction (XRD) pattern of CdSe cores is consistent with cubic CdSe structure (JCPDS card No. 19-0191), while the XRD pattern of CdSe/CdS QDs moves gradually toward higher angle (Figure S2), well catering to previous reports of forming CdS shell on CdSe core.[42,43] Figure S3 compares the room temperature Raman spectra of the two kinds of QDs, besides the shift of Raman peak of CdSe QDs at ~197 cm^{-1} to 225 cm^{-1} due to the compressive and tensile train of CdSe cores,[44] an additional peak (~294 cm^{-1}) appears caused by the growth of CdS shell. The exact surface stoichiometry of the obtained CdSe/CdS QDs is determined by X-ray photoelectron spectroscopy (XPS) measurements. As compared with the mother CdSe core, the ratio of surface Se atom decreased from 12.98% to 3.21%, and the ratio of surface S increased from 37.99% to 60.21%, see details in Table S1-S2. These results also confirm the growth of CdS shell on the surface of CdSe core to give corresponding core/shell QDs. On the other hand, colloidal Pt-nanoparticles are synthesized by reducing platinum precursor with hydrogen gas in the presence of polyacrylate as ligands, see details in Supporting Information. The average size of the face-centered cubic Pt-nanoparticles is determined to be ~3.5 nm using TEM (Figure 1c and Figure S4a). Normalized Pt L_3-edge X-ray absorption near edge structure (XANES) features of Pt foil and Pt-nanoparticles are shown in Figure S5. Pt L_3-edge of Pt-nanoparticles exhibits a shift (~1.5 eV) in the absorption peak to higher energy than that of Pt foil, which advocates the presence of oxidized species on Pt-nanoparticle surface presumably due to the adsorption of oxygen atoms of polyacrylate. This assumption is also confirmed by XPS results. Two pairs of doublets are obtained after deconvolution from the signal of Pt-nanoparticles (Figure 1d), which can be ascribed to metallic Pt (70.5 eV for Pt $4f_{7/2}$ and 74.2 eV Pt $4f_{5/2}$) and Pt^{2+} species (72.2 eV for Pt $4f_{7/2}$ and 75.5 eV Pt $4f_{5/2}$).[45,46] Quantitative analysis shows that 94% of surface Pt atoms of Pt-nanoparticles exist in oxidized state and the other 6% surface Pt atoms exist in metallic state. According to literature report,[47] the presence of oxidized Pt species is a result of wrapping polyacrylate chain around Pt-nanoparticles *via* coordination between carboxyl group and surface Pt atoms, as shown in Figure S4b.

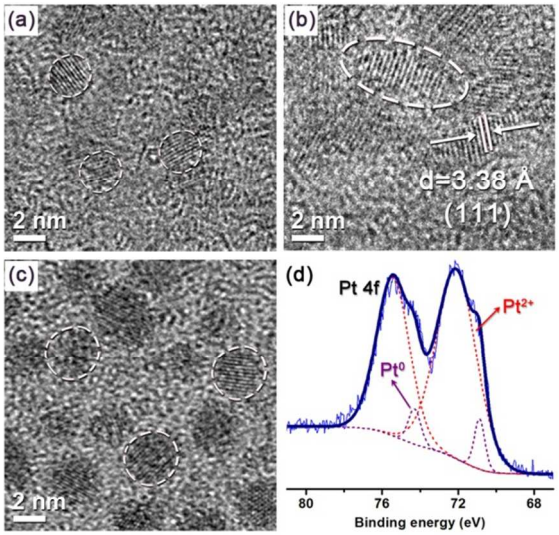

Figure 1. TEM images of CdSe QDs (a), CdSe/CdS QDs (b) and Pt-nanoparticles (c). (d) XPS result of Pt-nanoparticles.

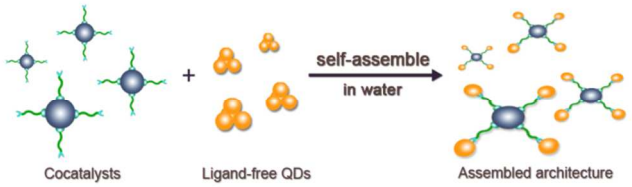

Scheme 1. Schematic illustration of the process of the self-assembled architecture between ligand-free QDs and Pt-nanoparticles in aqueous solution formed *in situ*.

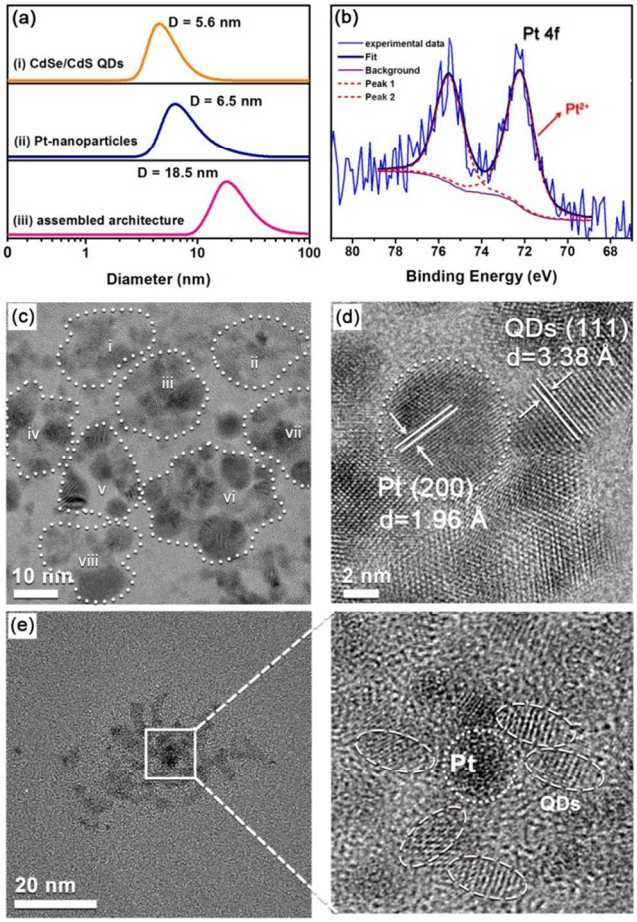

Figure 2. (a) DLS profiles of CdSe/CdS QDs, Pt-nanoparticles, and the assembled solution. (b) XPS spectrum of Pt-nanoparticles in the assembly. (c) TEM image of the assembled clusters of CdSe/CdS QDs and Pt-nanoparticles and (d) the corresponding high-resolution TEM image of assembled cluster (**vi**) in (**c**). (e) TEM image obtained at low concentration of the solution and the corresponding high-resolution TEM image of assembled cluster.

With CdSe/CdS QDs and Pt-nanoparticles in hand, the nanoparticle assembly is prepared through a very simple approach by dispersing the ligand-free CdSe/CdS QDs in 2.0 mL stock solution of colloidal Pt-nanoparticles. After 30 min ultrasonic treatment, QD/Pt-nanoparticle assembly is formed *in situ* as a transparent solution, which is stable for 12 h under darkness (Figure S6). Dynamic light scattering (DLS) indicates that CdSe/CdS QDs and Pt-nanoparticles are with a hydrodynamic size around 5.6 nm and 6.5 nm, both of which are larger than the TEM results due to the presence of surface ligands. The hydrodynamic size distribution of the obtained assembly is around 18.5 nm, apparently larger than that of CdSe/CdS QDs and Pt-nanoparticles alone, indicating the direct interaction between QDs and Pt-nanoparticles. The fact that no signals of metallic Pt are observed from the XPS spectrum of the assembly as compared with pure Pt-nanoparticles might suggest that the Pt-nanoparticles are closely surrounded by the QDs in the assembly (Figure 2b). For comparison, physical mixture of QDs and Pt-nanoparticles is analyzed using XPS at the same condition with QDs/Pt assembly. As shown in Figure S7, both metallic and oxidized Pt species are observed, indicating the disappearance of metallic Pt in Figure 2b is caused by the formation of nanoparticle assembly. Indeed, high-resolution TEM images directly verify the formation of assembly of CdSe/CdS QDs and Pt-nanoparticles in aqueous solution. As presented in Figure 2c, CdSe/CdS QDs and Pt-nanoparticles are closely interacted with each other to form assembled nanoclusters, denoted as (i) to (viii) in white circles with a diameter around 20 nm, which is highly consistent with DLS results. Figure 2d presents the corresponding high-resolution TEM image of cluster (vi) in Figure 2c, indicating that a single Pt-nanoparticle, with a lattice spacing of 1.96 Å for (200) plane, is surrounded by multiple CdSe/CdS QDs, with a lattice spacing of 3.38 Å for (111) plane, to form the self-assembled architecture of colloidal nanoparticles. Furthermore, TEM images obtained at low concentration of the solution confirm the presence of the assembled architecture (Figure 2e). As there are many vacant sites on the surface of ligand-free CdSe/CdS QDs, carboxylate group of polyacrylate on Pt-nanoparticles can readily coordinate with QDs on the vacant sites of cadmium ions with a binding constant of ~10^6 M^{-1},[48] which is a strong interaction but weaker than that of thiols (~10^9 M^{-1}).[49] Because of the stronger affinity of thiol group on QDs than that of carboxyl group (*vide ante*), MPA stabilized CdSe/CdS QDs, obtained through ligand-exchange method[50] (see Supporting Information for details), are well separated from Pt-nanoparticles due to the strong electrostatic repulsion in the mixture of aqueous solution, which leads to the collapse of the assembled architecture (Figure S8). Based on the above results, the picture of the formation process of the assembled architecture of CdSe/CdS QDs and Pt-nanoparticles is clear, as illustrated in Scheme 1. Due to the abundant carboxylate ligands on the surface of Pt-nanoparticles, multiple QDs can simultaneously interact with a single Pt-nanoparticle to form a self-assembled nanocluster.[51,52] Then, the self-assembled nanoclusters connect with each other by the same ligands to form dynamic networks. Though the exact coordination number of QDs to per Pt-nanoparticle can't be determined at this stage, the *in situ* assembled nanocluster, connecting ultra-small sized QDs and Pt-nanoparticles together to form an assembly, has been established. It is beneficial for shortening the distance between QDs and Pt-nanoparticles and in turn reducing the energy barrier of interfacial electron transfer for sure.

Visible-light induced H_2 evolution experiments. An initial photocatalytic H_2 production performance of the assembled architecture of CdSe/CdS QDs and Pt-nanoparticles is examined under visible-light irradiation. For comparison, the solar H_2 evolution of control system, in which MPA-

CdSe/CdS QDs and Pt-nanoparticles are individually separated from each other, is also studied under the identical condition. The solution was firstly deaereted by N_2 gas bubbling for 30 min before visible-light irradiation (450 nm), see details in Supporting Information. During a long period of 8 h, a total volume of 94 ± 1.5 mL (4183 ± 67 μmol) H_2 gas is produced from 5.0 mL solution under visible-light illumination (Figure 3a). A total TON of more than 16,400,000 mol H_2 (mol Pt-nanoparticle)$^{-1}$ is obtained, giving a turnover frequency (TOF) of ~570 s^{-1}. By employing 410 nm LEDs as the light source, the apparent quantum yield (AQY) of photocatalytic H_2 evolution in the first 30 min is determined to be ~43.7%. Taking incident photon loss caused by light scattering into consideration, the internal quantum yield (IQY) is estimated to ~65%, see details in Supporting Information. A comparison of the performance of solar H_2 evolution obtained here with literature reports is presented in Table S3. Under identical condition, however, only trace amount (~22 μmol h^{-1}) of molecular H_2 is produced when MPA stabilized CdSe/CdS QDs are employed as light absorbers (Figure 3a).

To investigate the influence of surface MPA, CdSe/CdS QDs with different numbers of MPA, from partial passivation to full coverage, were prepared for H_2 evolution. As shown in Figure S9 and Figure 3b, the amount of H_2 gas evolved in 1.0 h irradiation declined from ~780 μmol of ligand-free CdSe/CdS QDs to ~20 μmol of MPA-covered counterparts. Moreover, we found that removal of surface ligands from the as-prepared MPA-CdSe/CdS QDs revive the activity of solar H_2 evolution to ~748 ± 26 μmol, which is quite close to the value of ~780 ± 20 μmol of the initial ligand-free QDs. Surprisingly, the process of inhibiting and reviving the activity of solar H_2 evolution of CdSe/CdS QDs can be repeated for multiple times (Figure 3b), see experimental details in Figure S10. All of the observations indicate that the skeleton structure of CdSe/CdS QDs is preserved during the process of surface modification. The low efficiency of photocatalytic H_2 evolution for MPA-QDs can be explained by the fact that, at the early stage, thiol group of MPA occupies the sites of surface cadmium and blocks the assembly of Pt-nanoparticles with QDs, which results in the separation of QDs with cocatalysts. As a result, the energy barrier of interfacial electron transfer through a diffusion-controlled process is increased, leading to significant decrease in the rate of solar H_2 production. Further, during visible-light irradiation, the surface MPA may dissociate from QD surface, resulting in the self-aggregation and further photo-corrosion of QD itself.[53] As a result, the enhancement of solar H_2 evolution is significantly inhibited using MPA-QDs as light absorbers.

To examine whether the enhanced activity of solar H_2 evolution comes from band bending of QDs with varied surface ligands, UV-vis absorption spectra and valence band XPS measurements are carried out. CdSe/CdS QDs, stabilized by sulfide, MPA, and polyacrylate, show identical first exciton (1S) peak at 470 nm (Figure S11a), indicating the unchanged band gap of QDs.[54] Together with their very similar valence band maximum (E_{vb}) located at ~0.92 V, ~0.86 V and ~0.90 V *vs* normal hydrogen electrode (NHE), respectively (Figure S11b-11d), it's reasonable to conclude that both valence band and conduction band of CdSe/CdS QDs nearly keep unchanged as changing the surface ligands. That is to say, the driving force of QDs with ligands mentioned above for photocatalytic H_2 evolution is nearly the same.

In addition, the rate of H_2 evolution is found to depend on the concentration of Pt-nanoparticles (Figure 3c). At the lower concentration, the decrease in the rate of H_2 evolution is due to lack of enough active sites of cocatalyst for proton reduction, whereas at the higher concentration, the light-shielding effect of excessive amount of Pt-nanoparticles is operative largely. Control experiments show that QDs, Pt-nanoparticles and sacrificial reagent are necessary for solar H_2 generation. In the absence of Pt, negligible H_2 is produced, indicating the poor self-catalytic performance of CdSe/CdS QDs (Figure S12). In the absence of sacrificial reagent, no H_2 is produced by the assembly of QDs and Pt-nanoparticles (Figure S13). Even introduction of excess polyacrylate into the solution cannot evolve H_2 gas, suggesting that polyacrylate is unlikely to serve as an electron donor in the course of photocatalytic cycle. The other sacrificial reagents are also examined. As shown in Figure S14, ascorbic acid and isopropyl alcohol (IPA), deteriorate H_2 evolution because acidic condition favors the protonation of carboxyl group, which in turn causes the collapse of the assembled framework.

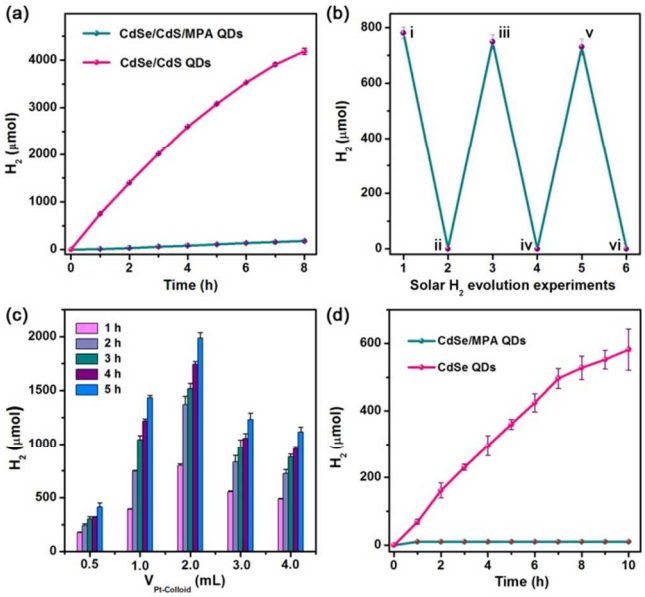

Figure 3. (a) Photocatalytic H_2 evolution of CdSe/CdS QDs/Pt-nanoparticle assembly and individually separated system using MPA stabilized counterparts. (b) Solar H_2 evolution of ligand-free CdSe/CdS QDs (i, iii and v) and MPA-CdSe/CdS QDs (ii, iv and vi) under identical conditions. (c) The variation of the rate of solar H_2 evolution with different amount of Pt-nanoparticles. (d) Solar H_2 evolution experiments of CdSe QDs/Pt-nanoparticles assembly and control experiment. The concentrations of QDs and Pt-nanoparticles are 5.0×10^{-6} mol·L^{-1} and 5.0×10^{-8} mol·L^{-1} respectively in a total volume of 5.0 mL solution containing 4.0 mL water and 1.0 mL Et_3N. Error bars represent mean ±s.d. of at least three independent experiments.

To strengthen the vital role of polyacrylate ligand as an effective linkage to bind QDs and Pt-nanoparticles, and simultaneously reduce the formation of trap states on the surface of QDs, Pt-nanoparticles with an average diameter of ~3.0

nm (Figure S15a-15c), similar with the size of Pt-nanoparticles used in the assembled system, is successfully attached on the surface of CdSe/CdS QDs using a reported photodeposition method.[55] As shown in Figure S15d, CdSe/CdS/Pt heterostructures show much lower efficiency and stability of solar H_2 evolution than the corresponding QD/Pt-nanoparticle assembly. It is accepted that the electron transfer rate is significantly influenced by the distance (*d*) between electron donor and acceptor.[56] Although facile photo-induced electron transfer can be achieved due to the direct contact between QD and Pt in the heterostructured materials, the trap states formed on the surface of relatively vulnerable QDs are unfavorable for H_2 evolution. In QDs/Pt assembly, the polyacrylate linkages shorten the distance between QDs and Pt-nanoparticles for ensuring fast electron transfer, and simultaneously keep the surface of QDs intact to a great extent due to the stabilization property of carboxyl group.[57] Further increasing the chain length of polyacrylate exerts negative effects on the performance of solar H_2 evolution under the same condition (Figure S16a), probably due to the fact that the increased chain length of polyacrylate enlarges the average distance (*d*) between CdSe/CdS QDs and Pt-nanoparticles (Figure S16b).

Significantly, this is a universal approach to improve the interparticle electronic communication of other QDs between cocatalysts for enhanced solar H_2 evolution. Taking CdSe QDs as an example, a mixture of organic ligand (MPA) stabilized CdSe QDs and Pt-nanoparticles produces negligible amount of molecular H_2 (~9.6 μmol) in a course of 10 h with visible-light irradiation (Figure 3d). However, the assembled system of ligand-free CdSe QDs and Pt-nanoparticles with the assist of polyacrylate ligands produces a total volume of 13 ± 1.4 mL (582 ± 61 μmol) molecular H_2 from a volume of 5.0 mL solution during 10 h, about 60-fold to that of MPA-CdSe QDs under the identical condition (Figure 3d), which gives a TON of >2,800,000 per Pt-nanoparticle, corresponding to a TOF of >77 s^{-1}. The better performance of H_2 evolution of CdSe/CdS QDs is due to its advantages in light absorption at 450 nm and charge separation compared with CdSe counterparts.[58]

Kinetics of interparticle electron transfer. The self-assembled architectures of QDs and Pt-nanoparticles simply jointed by polyacrylate have been achieved. Next, we employ steady-state emission quenching, time-resolved emission decay, femtosecond transient absorption (TA) spectroscopy and X-ray transient absorption (XTA) spectroscopy to evaluate the interparticle electronic communication. As shown in Figure 4a, colloidal Pt-nanoparticles exhibit negligible absorbance above 450 nm in water. CdSe/CdS QDs alone show a first exciton (1S) peak at 470 nm and two distinct emission bands, a narrow band-edge emission at 500 nm and a broad trap-state emission around 670 nm. In the presence of Pt-nanoparticles, the emission of CdSe/CdS QDs is significantly quenched, with a corresponding quenching constant of ~10^{14} M^{-1} s^{-1} (Figure S17), which is ~10^4 order higher than the upper limit for diffusion-limited process. Simultaneously, the emission lifetime of CdSe/CdS QDs dramatically decreased in the presence of Pt-nanoparticles (Figure 4b), indicating a faster decay of excitons of excited CdSe/CdS QDs. Since the lack of spectral overlap between the emission of CdSe/CdS QDs and the absorption of Pt-nanoparticles, energy transfer process is unlikely to occur, the interfacial electron transfer from excited CdSe/CdS QDs to Pt-nanoparticle is therefore responsible for the emission quenching and lifetime decay.

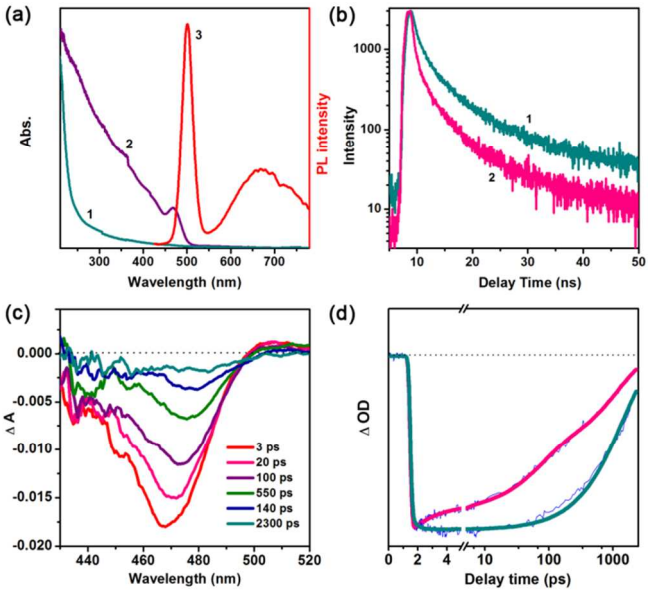

Figure 4. (a) UV-vis absorption spectra of colloidal Pt-nanoparticles (5.0×10^{-8} mol·L^{-1}) (line 1) and colloidal CdSe/CdS QDs (5.0×10^{-6} mol·L^{-1}) (line 2) in aqueous solution, and the emission spectrum of CdSe/CdS QDs (5.0×10^{-6} mol·L^{-1}) (line 3). (b) Time-resolved emission decay of CdSe/CdS QDs (5.0×10^{-6} mol·L^{-1}) in the presence (line 2) and absence (line 1) of Pt-nanoparticles (5.0×10^{-8} mol·L^{-1}). (c) Femtosecond TA spectra of CdSe/CdS QDs (1.4×10^{-4} mol·L^{-1}) in aqueous solution at indicated delay times after 400 nm laser excitation (3 to 2300 ps) in the presence of colloidal Pt-nanoparticles (1.4×10^{-6} mol·L^{-1}). (d) Comparison of the TA kinetics of CdSe/CdS QDs excited state at 470 nm in the absence (cyan line) and presence (pink line) of colloidal Pt-nanoparticles.

The exciton dynamics of CdSe/CdS QDs and the interparticle electron transfer kinetics from CdSe/CdS QDs to Pt-nanoparticles were further determined by femtosecond TA spectroscopy. After 400 nm laser excitation, TA spectra of bare CdSe/CdS QDs measured at indicated delay times are presented in Figure S18. The 1S (470 nm) exciton bleach recovers only ~12.5% in a 100 ps time window, indicating long-lived excitons and negligible exciton-exciton annihilation. In sharp contrast, the bleach absorption of CdSe/CdS QDs at 470 nm within the same time scale (100 ps) recovers almost ~66.5% in the presence of Pt-nanoparticles (Figure 4c). The small redshifts in the bleach band with increasing delay times can be explained by Stark effect.[59] The faster exciton bleach recovery of CdSe/CdS QDs indicates the accelerated exciton decay kinetics of CdSe/CdS QDs. Fitting the TA kinetic of CdSe/CdS QDs at 470 nm in the presence of Pt-nanoparticles yields the amplitude-weighted electron-transfer time (τ_a) as ~65 ps (Figure 4d),[60] see details in Table S4. This value caters the time scale of interparticle electron transfer in nanoparticle assembly,[61] which greatly exceeds the diffusion-controlled limit of interfacial electron transfer process.

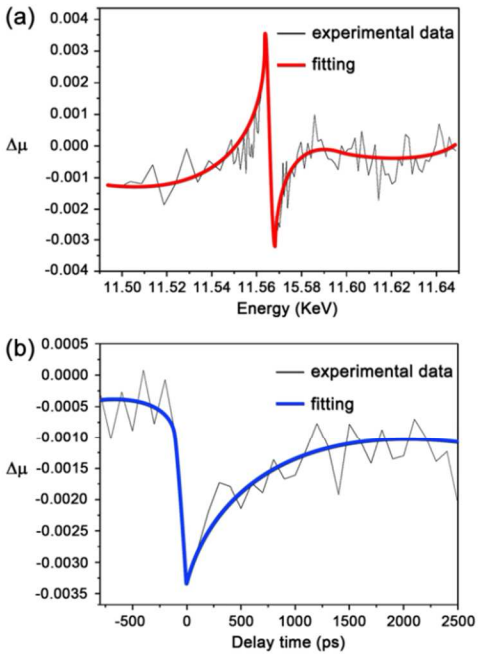

Figure 5. (a) Difference XANES spectra of Pt-L_3 absorption edge from the assembly of CdSe/CdS QDs and Pt-nanoparticles at laser-on and laser-off (laser 118 μJ/pulse) integrated up to 60 ps. (b) Decay scan of Pt-L_3 absorption edge at 11.568 KeV after 400 nm laser excitation.

The ultrafast kinetics of the photo-induced interparticle electron transfer from CdSe/CdS QDs to Pt-nanoparticles is further supported by X-ray transient absorption (XTA) spectra, an emerging and powerful technique to investigate photochemical processes in artificial photosynthesis recently.[62-64] Figure 5a shows the difference XANES spectra of Pt-L_3 absorption edge (excited minus unexcited in Figure S19) obtained from the assembly of CdSe/CdS QDs and Pt-nanoparticles with laser-on and laser-off at a delay time of 60 ps. In spite of the small difference in spectra, an edge shift feature shows the change of oxidation state at the Pt center. More importantly, the time scale of delay time in XTA is highly consistent with the result of ultra-fast TA measurement (~65 ps), indicating that the partial reduction of surface Pt atoms of Pt-nanoparticles is resulted from the interparticle electron transfer from CdSe/CdS QDs to Pt-nanoparticles. Figure 5b is the decay scan of Pt-L_3 absorption edge at 11.568 KeV in Figure 5a after laser excitation of 60 ps, indicating the discharge kinetics of electrons at the electrolyte interface. Though the XTA signal doesn't recover fully within the present time range, possibly due to the fact that some electrons are trapped on the surface of Pt-nanoparticles, this preliminary study provides the first example of employing XTA to investigate the charge carrier kinetics in nanoparticle assembly, and shows great potential application of XTA in solar H_2 generation study.

Energy-level alignment provides further thermodynamic evidences for the interparticle electron transfer. The size of CdSe QDs used here is ~2.0 nm, corresponding to a band gap of 2.65 eV using *Tauc* plot, as illustrated in Figure S20. Then, the conduction band and valence band potentials of CdSe QDs can be determined as -1.42 V and 1.23 V, respectively, *versus* normal hydrogen electrode (NHE)[65,66] (Figure 6a). Herein, Pt-nanoparticles can act as a sink for accepting multiple photoelectrons that is beneficial for promoting charge separation.[67] The process of electron transfer from the conduction band of CdSe QDs to the Femi level of Pt-nanoparticles is thermodynamically feasible. Although most of surface platinum atoms of Pt-nanoparticles are in the form of PtO_x (x<1) due to the coordination of carboxyl group, the HER performance is comparable to that of the benchmark of conventional metallic Pt.[68] Compared with diffusion-controlled ET between individually separated QDs and co-catalysts, the ligand-assisted *in situ* assembly of QDs and Pt-nanoparticles in aqueous solution can decrease the interparticle distance and increase the mutual communication between the two species, and in turn guarantee more facile and fast interparticle charge transfer. The surrounding multiple QDs to a single catalyst in the assembled nanoclusters ensures electron migration to cocatalyst consecutively, which presents a strategy to combine single photon/electron events with multi-electron redox reaction of molecular H_2 production (Figure 6b). Additionally, CdSe/CdS counterparts present better visible-light response and charge-separation properties than CdSe QDs. The added values make the assembled architecture of CdSe/CdS QDs/Pt-nanoparticles exceptional for solar H_2 evolution.

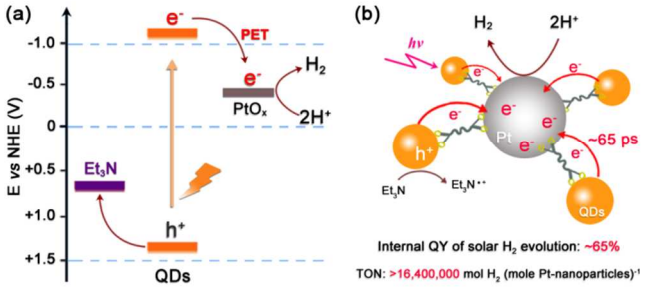

Figure 6. (a) The band positions of CdSe QDs and corresponding processes of charge transfer in the assembly. (b) Schematic illustration of the assembly of QDs/Pt-nanoparticles and the corresponding solar H_2 evolution process.

CONCLUSION

In summary, we have demonstrated that simple fabrication of QDs and Pt-nanoparticles into an *in situ* assembled framework is a promising way to increase the interparticle interaction, leading to ultrafast electron transfer between the ultra-small nanoparticles that is generally diffusion-controlled with an upper limit of 10^{10} M^{-1} s^{-1}. Unlike most state-of-the-art approaches, the approach does not rely on further structure modification of colloidal QDs or introduction of a third component of electron mediator but on the self-assembling way of QDs and cocatalysts directly connected by molecular linkers. This concept can also combine single photon/electron events with multi-electron redox reactions to increase the performance of solar H_2 evolution to give a quantum yield of ~65% and a TON value of >16,400,000 based on Pt-nanoparticles. This simple and promising way for effective interfacial charge separation and migration of ultra-small sized nanoparticles paves a brand

new avenue for designing highly efficient artificial photosystems for practical applications.

ASSOCIATED CONTENT

Supporting Information

This material is available free of charge via the Internet at http://pubs.acs.org.

AUTHOR INFORMATION

Corresponding Author

E-mail: lzwu@mail.ipc.ac.cn; Telephone: (+86) 10-8254-3580.

Notes

The authors declare no competing financial interests.

ACKNOWLEDGMENT

We are grateful for the financial support from the Ministry of Science and Technology of China (2013CB834505, 2014CB239402 and 2013CB834804), the National Natural Science Foundation of China (91027041, 21390404, 21603248 and 51373193), and the Strategic Priority Research Program of the Chinese Academy of Science (XDB17030300), and the Chinese Academy of Sciences. We especially thank Beijing Synchrotron Radiation Facility (BSRF, Beamline 1W2B) for providing the beam time of X-ray absorption measurements. Meanwhile, this research used resources of the Advanced Photon Source, a U.S. Department of Energy (DOE) Office of Science User Facility operated for the DOE Office of Science by Argonne National Laboratory under Contract No. DE-AC02-06CH11357.

REFERENCES

(1) Gray, H. B. *Nat. Chem.* **2009**, *1*, 7-7.
(2) Wang, W.; Chen, J.; Li, C.; Tian, W. *Nat. Commun.* **2014**, *5*, 4647.
(3) Nocera, D. G. *Energy Environ. Sci.* **2010**, *3*, 993.
(4) Han, Z.; Qiu, F.; Eisenberg, R.; Holland, P. L.; Krauss, T. D. *Science* **2012**, *338*, 1321.
(5) Bi, W.; Li, X.; Zhang, L.; Jin, T.; Zhang, L.; Zhang, Q.; Luo, Y.; Wu, C.; Xie, Y. *Nat. Commun.* **2015**, *6*, 8647.
(6) Armstrong, F. A. *Science* **2013**, *339*, 658.
(7) Simon, T.; Bouchonville, N.; Berr, M. J.; Vaneski, A.; Adrović, A.; Volbers, D.; Wyrwich, R.; Döblinger, M.; Susha, A. S.; Rogach, A. L.; Jäckel, F.; Stolarczyk, J. K.; Feldmann, J. *Nat. Mater.* **2014**, *13*, 1013.
(8) Weingarten, A. S.; Kazantsev, R. V.; Palmer, L. C.; McClendon, M.; Koltonow, A. R.; SamuelAmanda, P. S.; Kiebala, D. J.; Wasielewski, M. R.; Stupp, S. I. *Nat. Chem.* **2014**, *6*, 964-970.
(9) Tian, J.; Xu, Z.-Y.; Zhang, D.-W.; Wang, H.; Xie, S.-H.; Xu, D.-W.; Ren, Y.-H.; Wang, H.; Liu, Y.; Li, Z.-T. *Nat. Commun.* **2016**, *7*, 11580.
(10) Schulze, M.; Kunz, V.; Frischmann, P. D.; Würthner, F. *Nat. Chem.* **2016**, *8*, 576.
(11) Jian, J.-X.; Liu, Q.; Li, Z.-J.; Wang, F.; Li, X.-B.; Li, C.-B.; Liu, B.; Meng, Q.-Y.; Chen, B.; Feng, K.; Tung, C.-H.; Wu, L.-Z. *Nat. Commun.* **2013**, *4*, 2695.
(12) Chen, Y.; Zhao, S.; Wang, X.; Peng, Q.; Lin, R.; Wang, Y.; Shen, R.; Cao, X.; Zhang, L.; Zhou, G.; Li, J.; Xia, A.; Li, Y. *J. Am. Chem. Soc.* **2016**, *138*, 4286.
(13) Kalisman, P.; Nakibli, Y.; Amirav, L. *Nano Lett.* **2016**, *16*, 1776.
(14) Kim, D.; Sakimoto, K. K.; Hong, D.; Yang, P. *Angew. Chem. Int. Ed.* **2015**, *54*, 3259.
(15) Smith, A. M.; Nie, S. *Acc. Chem. Res.* **2009**, *43*, 190.
(16) Talapin, D. V.; Lee, J.-S.; Kovalenko, M. V.; Shevchenko, E. V. *Chem. Rev.* **2009**, *110*, 389.
(17) Wu, L.-Z.; Chen, B.; Li, Z.-J.; Tung, C.-H. *Acc. Chem. Res.* **2014**, *47*, 2177.
(18) Han, Z.; Eisenberg, R. *Acc. Chem. Res.* **2014**, *47*, 2537.
(19) Artero, V.; Chavarot-Kerlidou, M.; Fontecave, M. *Angew. Chem. Int. Ed.* **2011**, *50*, 7238.
(20) Luo, S.-P.; Mejía, E.; Friedrich, A.; Pazidis, A.; Junge, H.; Surkus, A.-E.; Jackstell, R.; Denurra, S.; Gladiali, S.; Lochbrunner, S.; Beller, M. *Angew. Chem. Int. Ed.* **2013**, *52*, 419.
(21) Maitra, U.; Gupta, U.; De, M.; Datta, R.; Govindaraj, A.; Rao, C. N. R. *Angew. Chem. Int. Ed.* **2013**, *52*, 13057.
(22) Wang, C.; deKrafft, K. E.; Lin, W. *J. Am. Chem. Soc.* **2012**, *134*, 7211.
(23) Zheng, Y.; Lin, L.; Wang, B.; Wang, X. *Angew. Chem. Int. Ed.* **2015**, *54*, 12868.
(24) Tarafder, K.; Surendranath, Y.; Olshansky, J. H.; Alivisatos, A. P.; Wang, L.-W. *J. Am. Chem. Soc.* **2014**, *136*, 5121.
(25) Zhu, H.; Yang, Y.; Lian, T. *Acc. Chem. Res.* **2012**, *46*, 1270.
(26) Knowles, K. E.; Malicki, M.; Weiss, E. A. *J. Am. Chem. Soc.* **2012**, *134*, 12470.
(27) Brown, K. A.; Wilker, M. B.; Boehm, M.; Dukovic, G.; King, P. W. *J. Am. Chem. Soc.* **2012**, *134*, 5627.
(28) Zhu, H.; Song, N.; Lv, H.; Hill, C. L.; Lian, T. *J. Am. Chem. Soc.* **2012**, *134*, 11701.
(29) Yu, S.; Li, Z.-J.; Fan, X.-B.; Li, J.-X.; Zhan, F.; Li, X.-B.; Tao, Y.; Tung, C.-H.; Wu, L.-Z. *ChemSusChem* **2015**, *8*, 642.
(30) Xiang, Q.; Yu, J.; Jaroniec, M. *J. Am. Chem. Soc.* **2012**, *134*, 6575.
(31) Huang, J.; Mulfort, K. L.; Du, P.; Chen, L. X. *J. Am. Chem. Soc.* **2012**, *134*, 16472.
(32) Xu, Y.; Ye, Y.; Liu, T.; Wang, X.; Zhang, B.; Wang, M.; Han, H.; Li, C. *J. Am. Chem. Soc.* **2016**, *138*, 10726.
(33) Li, C.-B.; Li, Z.-J.; Yu, S.; Wang, G.-X.; Wang, F.; Meng, Q.-Y.; Chen, B.; Feng, K.; Tung, C.-H.; Wu, L.-Z. *Energy Environ. Sci.* **2013**, *6*, 2597.
(34) Yan, H.; Yang, J.; Ma, G.; Wu, G.; Zong, X.; Lei, Z.; Shi, J.; Li, C. *J. Catal.* **2009**, *266*, 165.
(35) Li, Z.-J.; Li, X.-B.; Wang, J.-J.; Yu, S.; Li, C.-B.; Tung, C.-H.; Wu, L.-Z. *Energy Environ. Sci.* **2013**, *6*, 465.
(36) Li, X.-B.; Li, Z.-J.; Gao, Y.-J.; Meng, Q.-Y.; Yu, S.; Weiss, R. G.; Tung, C.-H.; Wu, L.-Z. *Angew. Chem. Int. Ed.* **2014**, *53*, 2085.
(37) Hohmann-Marriott, M. F.; Blankenship, R. E. *Annu. Rev. Plant Biol.* **2011**, *62*, 515.
(38) Frischmann, P. D.; Mahata, K.; Wurthner, F. *Chem. Soc. Rev.* **2013**, *42*, 1847.
(39) Li, J. J.; Wang, Y. A.; Guo, W.; Keay, J. C.; Mishima, T. D.; Johnson, M. B.; Peng, X. *J. Am. Chem. Soc.* **2003**, *125*, 12567.
(40) Zeng, Q.; Kong, X.; Sun, Y.; Zhang, Y.; Tu, L.; Zhao, J.; Zhang, H. *J. Phys. Chem. C* **2008**, *112*, 8587.
(41) Peng, X.; Schlamp, M. C.; Kadavanich, A. V.; Alivisatos, A. P. *J. Am. Chem. Soc.* **1997**, *119*, 7019.
(42) Silva, A. C. A.; Neto, E. S. F.; da Silva, S. W.; Morais, P. C.; Dantas, N. O. *J. Phys. Chem. C* **2013**, *117*, 1904.
(43) Silva, A. C. A.; da Silva, S. W.; Morais, P. C.; Dantas, N. O. *ACS Nano* **2014**, *8*, 1913.
(44) Tschirner, N.; Lange, H.; Schliwa, A.; Biermann, A.; Thomsen, C.; Lambert, K.; Gomes, R.; Hens, Z. *Chem. Mater.* **2011**, *24*, 311.
(45) Wang, Y.; Wang, Y.; Xu, R. *J. Phys. Chem. C* **2012**, *117*, 783.
(46) Nie, R.; Wang, J.; Wang, L.; Qin, Y.; Chen, P.; Hou, Z. *Carbon* **2012**, *50*, 586.
(47) Tongsakul, D.; Nishimura, S.; Ebitani, K. *J. Phys. Chem. C* **2014**, *118*, 11723.

(48) Cui, S.-C.; Tachikawa, T.; Fujitsuka, M.; Majima, T. *J. Phys. Chem. C* **2010**, *114*, 1217.
(49) Koole, R.; Schapotschnikow, P.; de Mello Donegá, C.; Vlugt, T. J. H.; Meijerink, A. *ACS Nano* **2008**, *2*, 1703.
(50) Aldana, J.; Lavelle, N.; Wang, Y.; Peng, X. *J. Am. Chem. Soc.* **2005**, *127*, 2496.
(51) Zotti, G.; Vercelli, B.; Berlin, A.; Chin, P. T. K.; Giovanella, U. *Chem. Mater.* **2009**, *21*, 2258.
(52) Anderson, N. C.; Hendricks, M. P.; Choi, J. J.; Owen, J. S. *J. Am. Chem. Soc.* **2013**, *135*, 18536.
(53) Aldana, J.; Wang, Y. A.; Peng, X. *J. Am. Chem. Soc.* **2001**, *123*, 8844.
(54) Sapra, S.; Sarma, D. D. *Phys. Rev. B* **2004**, *69*, 125304.
(55) Dukovic, G.; Merkle, M. G.; Nelson, J. H.; Hughes, S. M.; Alivisatos, A. P. *Adv. Mater.* **2008**, *20*, 4306.
(56) Hutchison, G. R.; Ratner, M. A.; Marks, T. J. *J. Am. Chem. Soc.* **2005**, *127*, 16866.
(57) Liu, Y.; Kim, M.; Wang, Y.; Wang, Y. A.; Peng, X. *Langmuir* **2006**, *22*, 6341.
(58) Eshet, H.; Grünwald, M.; Rabani, E. *Nano Lett.* **2013**, *13*, 5880.
(59) Zhu, H.; Song, N.; Rodríguez-Córdoba, W.; Lian, T. *J. Am. Chem. Soc.* **2012**, *134*, 4250.
(60) Zhu, H.; Song, N.; Lian, T. *J. Am. Chem. Soc.* **2010**, *132*, 15038.
(61) Kamat, P. V.; Shanghavi, B. *J. Phys. Chem. B* **1997**, *101*, 7675.
(62) Chen, L. X.; Zhang, X. *J. Phys. Chem. Lett.* **2013**, *4*, 4000.
(63) Moonshiram, D.; Gimbert-Suriñach, C.; Guda, A.; Picon, A.; Lehmann, C. S.; Zhang, X.; Doumy, G.; March, A. M.; Benet-Buchholz, J.; Soldatov, A.; Llobet, A.; Southworth, S. H. *J. Am. Chem. Soc.* **2016**, *138*, 10586.
(64) Li, Z.-J.; Zhan, F.; Xiao, H.; Zhang, X.; Kong, Q.-Y.; Fan, X.-B.; Liu, W.-Q.; Huang, M.-Y.; Huang, C.; Gao, Y.-J.; Li, X.-B.; Meng, Q.-Y.; Feng, K.; Chen, B.; Tung, C.-H.; Zhao, H.-F.; Tao, Y.; Wu, L.-Z. *J. Phys. Chem. Lett.* **2016**, 5253.
(65) Zhao, J.; Holmes, M. A.; Osterloh, F. E. *ACS Nano* **2013**, *7*, 4316.
(66) Li, X.-B.; Liu, B.; Wen, M.; Gao, Y.-J.; Wu, H.-L.; Huang, M.-Y.; Li, Z.-J.; Chen, B.; Tung, C.-H.; Wu, L.-Z. *Adv. Sci.* **2016**, *3*, 1500282.
(67) Cui, E.; Lu, G. *J. Phys. Chem. C* **2013**, *117*, 26415.
(68) Li, Y. H.; Xing, J.; Chen, Z. J.; Li, Z.; Tian, F.; Zheng, L. R.; Wang, H. F.; Hu, P.; Zhao, H. J.; Yang, H. G. *Nat. Commun.* **2013**, *4*, 2500.

TOC

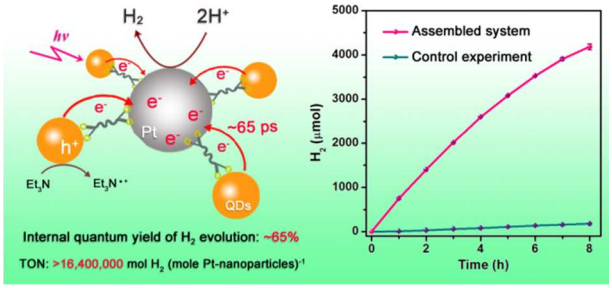
H2
2H+
hν
e-
h+
Pt
QDs
~65 ps
Et3N
Et3N+•
Internal quantum yield of H2 evolution: ~65%
TON: >16,400,000 mol H2 (mole Pt-nanoparticles)-1
Assembled system
Control experiment
H2 (μmol)
Time (h)
5000
4000
3000
2000
1000
0
0
2
4
6
8